Published in final edited form as:
J Immunol. 2009 November 15; 183(10): 6667. doi:10.4049/jimmunol.0900516.

Externally Triggered Egress Is the Major Fate of *Toxoplasma gondii* During Acute Infection[1]

Tadakimi Tomita[*], **Tatsuya Yamada**[*], **Louis M. Weiss**[*,†], and **Amos Orlofsky**[*,2]

[*]Department of Pathology Albert Einstein College of Medicine Bronx, NY USA

[†]Department of Medicine Albert Einstein College of Medicine Bronx, NY USA

Abstract

The apicomplexan parasite *Toxoplasma gondii* expands during acute infection via a cycle of invasion, intracellular replication and lytic egress. Physiological regulation has not yet been demonstrated for either invasion or egress. We now report that, in contrast to cell culture systems, in which egress occurs only after five or more parasite divisions (two to three days), intracellular residence is strikingly abbreviated in inflammatory cells *in vivo*, and early egress (after zero to two divisions) is the dominant parasite fate in acutely infected mice. Adoptive transfer experiments demonstrate rapid, reciprocal, kinetically uniform parasite transfer between donor and recipient compartments, with a half-life of approximately three hours. Inflammatory macrophages are major participants in this cycle of lytic egress and reinfection, which drives rapid macrophage turnover. Inflammatory triggering cells, principally macrophages, elicit egress in infected target macrophages, a process we term externally triggered egress (ETE). The mechanism of ETE does not require reactive oxygen or nitrogen species, the mitochondrial permeability transition pore, or a variety of signal transduction mediators, but is dependent on intracellular calcium and is highly sensitive to SB203580, an inhibitor of p38 MAP kinase as well as a related parasite-encoded kinase. SB203580 both inhibited the initiation of ETE and altered the progression of egress. Parasites recently completing a cycle of egress and reinfection were preferentially restricted *in vivo*, supporting a model in which ETE may favor host defense by a process of 'haven disruption'. ETE represents a novel example of interaction between a parasite infectious cycle and host microenvironment.

Keywords

Infections-Parasitic-Protozoan; Processes-Inflammation; Cells-Monocytes/Macrophages

Introduction

Toxoplasma gondii infection proceeds in two stages: an acute phase consisting of the rapid proliferation and dissemination of tachyzoites, followed by a chronic phase characterized by the formation of stable tissue cysts containing bradyzoites. The control of tachyzoite expansion,

[1]This study was supported by funds from National Institutes of Health grant AI-55358 to A.O and AI-39454 to L.M.W., and by the Flow Cytometry Core of the Center for AIDS Research (AI-51519).

2Corresponding author: orlofsky@aecom.yu.edu.

which is critical to host defense, depends on the ability of the developing immune response to limit parasite replication and survival (1). In addition to replication, however, the tachyzoite life cycle includes two essential events, invasion and egress, that offer potential points of regulatory control but have received comparatively less attention in this regard. This is especially true for egress: the extent to which this event is susceptible to physiological regulation is as yet unknown.

In cell culture systems, intracellular *Toxoplasma* progress through approximately 5 to 7 division cycles over 2 to 3 days before finally lysing the host cell in preparation for a new round of infection (2). However, egress can also be induced at earlier stages by agents such as calcium ionophores and dithiothreitol (3-8), or by cell death inducers such as perforin or fas ligand (9). These studies suggest that early egress can potentially be triggered by signals initiated by the host cell or its environment. Furthermore, a recent study indicates that inducible egress may be mechanistically distinct from the spontaneous egress observed in culture (10), lending further support to the notion that inducible egress may represent a distinct parasite function. However the question of whether such externally stimulated egress can occur in a physiological setting has not been examined. In this study we present evidence that inducible egress not only can occur physiologically but is in fact a dominant process in a model of acute toxoplasmosis.

Materials and Methods

Materials

The antibodies used were anti-F4/80-647 (Serotec), anti-CD11b-647, anti-B220-647, anti-Thy1.2-allophycocyanin and anti-1A8-phycoerythrin (Becton Dickinson). SB203580, U0126, Jnk inhibitor II, rottlerin, Go 6976 and BAPTA-AM were obtained from EMD. N-iminoethyl-l-lysine (L-NIL)[3], N-nitro-l-arginine methyl ester (L-NAME), N-acetylcysteine, pyridoxal-phosphate-6-azophenyl-2′,4′-disulfonate (PPADS), cyclosporine, fluridone and Accutase were from Sigma. Murine IFNγ was from Chemicon. CellTrace Far Red DDAO-SE (DDAO-SE) was from Invitrogen).

Parasites and mice

Parasites were maintained in human foreskin fibroblasts as described (11). The transgenic strain expressing GFP has been described (12). The yellow fluorescent protein (YFP)-expressing strain (13) was a kind gift of B. Striepen (Univ. of Georgia). The *in vitro* growth characteristics of the fluorescent strains were similar to wild-type. Mice (C57BL/6, 6 - 8 weeks old) were inoculated intraperitoneally with 0.2 ml PBS containing 2000 tachyzoites harvested from lysed cultures. Some experiments used mice expressing enhanced cyan fluorescent

[3]Abbreviations:

DAP	donor cell-associated parasite
DDAO-SE	CellTrace Far Red DDAO-SE
ECFP	enhanced cyan fluorescent protein
ETE	externally triggered egress
NDAP	non donor cell-associated parasite
L-NIL	N-iminoethyl-l-lysine
PEM	peritoneal exudate macrophages
WT-RH	wild-type RH
YFP	yellow fluorescent protein.

protein (ECFP) behind an actin promoter (stock number 4218, The Jackson Laboratory). Some samples for cytology were obtained from wildtype mice on a mixed C57BL/6 - 129/Sv background as previously described (14). All mice were maintained in a specific pathogen-free facility. All mouse studies were reviewed and approved by the Animal Institute Committee at the Albert Einstein College of Medicine. Peritoneal exudate macrophages (PEM) were prepared by lavage of mice injected 4 d previously with 1 ml of 3% thioglycolate broth (Difco). Stocks of frozen aliquots of PEM were generated from pooled lavage of at least 3 mice. PEM were also prepared from mice deficient in IFNγ receptor-1 (stock number 3288). Prior to infection, thawed PEM were cultured for 1 d in DMEM medium with 10% FBS.

Cytology

At various times post-infection, mice were sacrificed and the peritoneal cavity lavaged with ice-cold PBS/0.1% BSA. Cytospin preparations were fixed in methanol, dried, stained with a modified Wright's stain (LeukoStat, Fisher) and examined at 100x on a Zeiss Axioskop II. Microscope fields were chosen prior to observation and all infected mononuclear cells in the field were scored, except that vacuoles containing debris or degraded parasites (< 10% of total vacuoles) were excluded.

Adoptive exudate transfer

On day 5 post-infection, when ascites volume is approximately 1 ml, 0.1 ml of exudate was collected from all mice by paracentesis and immediately diluted with 4 ml chilled PBS containing 0.1% BSA, 1mM EDTA and 10U/ml heparin (buffer A), centrifuged at 150 g for 10 min and suspended in 100 μl PBS with 0.1% BSA. The samples were immediately analyzed by flow cytometry to determine percent cells infected, parasites/infected cell, and free parasites relative to total cells. Mice showing similar progression of toxoplasmosis by these criteria were selected as donor-host combinations. Donor mice were injected i.p. with 0.1ml Hoechst 33342 (200 μg/ml; Molecular Probes) and the abdomen briefly massaged. In comparison with the dye, genetic marking using CD45 or H2 alleles was less compatible with the use of fluorescent parasites and also provided inferior donor-host discrimination in a complex cell population (data not shown). Transgenic ECFP was used as a marker in some experiments, although it was not uniformly expressed in exudate cells (data not shown). After 1 h, donor mice were anesthetized with isoflurane and abdominal skin deflected. Donor exudate was gradually removed using a 0.5 cc syringe and 30g needle, and immediately transferred, with gradual expulsion to minimize shear, to the peritoneal cavity of host mice (0.1 ml per recipient), followed by brief abdominal massage. The time between exudate removal and completed transfer was 0.5 to 3 min. Remaining donor exudate was then diluted in buffer A and processed as above (0 h sample). The 0.5 cc syringe minimizes exposure of exudate to air. In some experiments, additional measures were taken to prevent exposure to high oxygen tension during transfer, but without noticeable effect on results. A comparison of autotransferred with unmanipulated animals showed no effect of exudate transfer upon the distribution of host parasite or host cell phenotypes (data not shown). At various times, 0.1 ml exudate was removed by paracentesis from host mice and diluted with chilled buffer A and processed as above. For phenotyping, samples were incubated on ice for 1 h in the presence of Fc block (Becton Dickinson) and antibody. Samples were either analyzed within 3 h on a LSRII flow cytometer, or else frozen at −80°C with 10% DMSO and thawed on ice prior to flow cytometry. In some experiments, propidium iodide was added to assess cell viability. Data were analyzed with FCS Express (De Novo Software) and SigmaPlot (Jandel).

For transfer of ^{51}Cr-labeled cells, PEM were suspended at 5×10^6/ml in HBSS/0.1% BSA, incubated with 100 μCi/ml ^{51}Cr-NaCrO4 (PerkinElmer) at 37° C for 45 min, washed three times in PBS/0.1% BSA and injected i.p. (1×10^6 cells in 0.1 ml). After 9 h, the thoracic viscera

(including the lymph nodes that drain the peritoneal cavity) were removed and counted in a gamma counter.

In vitro assays

For *ex vivo* egress assay, donor and host infected mice were prepared as above. Donor mice were labeled *in situ* with either Hoechst 33342 or 125 μl DDAO-SE (180 μg/ml), a far red-emitting dye similar to CFSE (Molecular Probes). After mice were sacrificed, exudates were obtained immediately by paracentesis, washed and suspended at original volume with cold RPMI medium containing 25 mM HEPES pH 7.4, 1mM EDTA, 10 U/ml heparin and 10% FBS (assay medium). In some cases, exudates were not washed but instead combined with 0.1 volume of 200 mM HEPES pH7.4, 10 mM EDTA and 100 U/ml heparin ('whole exudate'). Exudates were mixed and incubated at 37°C for 1.5 h in either microcentrifuge tubes or non-adherent 96-well plates (UltraLow, Corning). Samples were fixed in paraformaldehyde, combined with fluorescent beads (6.0 μm, 620 nm emission, Molecular Probes) to normalize sample volumes, and then analyzed by flow cytometry.

For timelapse imaging, 2×10^5 PEM were seeded in coverslip-thick glass 8-well chambers (Nunc) and infected with YFP-RH at moi = 0.3. The medium was replaced with 0.2 ml HEPES-buffered RPMI with 10% FBS, and the vessel placed in a temperature-controlled forced air chamber mounted on an Olympic IX70 microscope in the Analytical Imaging Facility of the Albert Einstein College of Medicine. Exudate cells (1×10^7/ml) were prepared on ice as described above from mice infected with wild-type RH strain (WT-RH). Chamber wells received 0.2 ml of either medium or exudate that had been briefly warmed to 37°C prior to addition. In some cases, exudate was mixed with 0.02 volume of either DMSO or 1 mM SB203580 immediately before addition Images were collected at 10 min intervals for 8 fields / well at 6 focal planes. Data were analyzed using ImageJ, and images generated with Photoshop.

For standard assay of externally triggered egress (ETE assay), PEM were infected overnight with YFP-RH in non-adherent dishes (moi of 0.2 - 1) and then labeled with 5 μM DDAO-SE for 1 h in medium containing 10% FBS. Labeled PEM (8×10^4 per well in 100 μl) were placed in non-adherent 96-well plates. Washed exudate cells were prepared as described above from WT-RH-infected mice. Wells containing labeled PEM received 0.1 ml of either medium or a suspension (4×10^6/ml in assay medium) of exudate cells, uninfected PEM, or WT-RH-infected PEM. In some experiments, in order to determine the basal egress in the absence of exudate cells, the labeled PEM were first diluted 1:9 with a suspension (at identical cell concentration) of unlabeled WT-RH-infected PEM, and then combined with exudate or additional PEM as above. The cell mixtures were placed in a 37°C incubator for 1 - 1.5 h, fixed with paraformaldehyde and analyzed by flow cytometry after the addition of fluorescent beads.

Depletion of exudate cells

Exudate from WT-RH-infected mice was diluted with Hank's saline containing 0.1% BSA and 1 mM EDTA. Exudate cells were washed and incubated for 30 min on ice with either anti-1A8-phycoerythrin, anti-F4/80-647, the combination of anti-F4/80-647 and anti-CD11b-phycoerythrin, or the combination of anti-1A8-phycoerythrin, anti-Thy1.2-allophycocyanin and anti-B220-647. The cells were washed and then incubated with anti-rat-IgG Dynabeads (Dynal) for 30 min. The cells were either exposed or not (mock-depleted) to a Dynal MPC-S magnet for 10 min, spun, and resuspended in assay buffer at 1×10^7/ml.

To deplete total host cells and enrich extracellular parasites, exudates from YFP-RH-infected mice were washed twice in assay buffer, pooled and 0.8 ml aliquots (3×10^7 cells/ml) placed in microcentrifuge tubes on ice. Some samples were then spun for 2 min in a Fisher 59A swing-out microcentrifuge in a cold room at a setting of 1.2 (approximately 100 g). Supernatant was

collected from spun samples. Aliquots of the samples were fixed for flow cytometry and the remainder briefly warmed before transfer (0.1 ml) to host mice.

Results

Intravacuolar parasite content in acute toxoplasmosis is consistent with early egress

Peritoneal inoculation of mice with 10^2 - 10^3 RH tachyzoites generates a progressive infection with a steadily increasing parasite burden that is predominantly localized to the peritoneal cavity, with involvement of adjacent sites (15-19). The inflammatory response in the peritoneum is characterized by the formation of ascites with a massive influx of monocytes and neutrophils approximately 3 to 4 days post-infection and is maintained for 3 to 4 days until the death of the host (17,20). In the course of studies employing this model, we noticed that peritoneal macrophages collected from mice during the peak period of inflammation rarely had parasitophorous vacuoles containing more than eight parasites, and we undertook to investigate whether early egress might account for this observation.

As a first step, we examined the extent of intravacuolar parasite proliferation in macrophages from mice acutely infected with *T. gondii* RH. Counts were performed by cytological examination of lavage samples (Fig. 1A) collected from mice that had entered peak inflammation (4 to 5 days post-infection), but did not yet exhibit signs of morbidity. Each intracellular parasite was assigned a 'proliferation value' P equal to the number of divisions completed by that parasite in that cell (for example, in a vacuole with three parasites, two are assigned P = 2 and one is assigned P = 1). The observed distribution of P was compared to two theoretical distributions representing alternative models of egress regulation (Fig. 1B). Both models assume that the distribution is asynchronous (time-invariant), that replication cycles are of constant length, that egress is unbiased with respect to parasite cell cycle stage (so that egress occurs, on average, at the midpoint of a cycle), and that the interval between egress and reinvasion is negligible (confirmed below).

Under the first model (conventional or proliferation - dependent egress), egress occurs at a fixed value c of P; that is, egress requires a certain number of parasite divisions. In this case, the time-invariant distribution is that in which the fraction of parasites is constant over P, except reduced by half for P = 0 and P = c, since egress is at mid-cycle (dashed line in Fig. 1B, illustrated for egress at P = 5). In the second model ('probabilistic egress'), egress occurs with equal probability at all P, consistent with an egress signal that is independent of parasite proliferation. Under this model, the distribution can be derived by iteration (beginning with a synchronous infection), and is given by $f_0 = 0.5q$ and $f_n = 0.5(q(1-q)^n + q(1-q)^{n-1})$ for $n > 0$, where f_n is the fraction of parasite for which P = n, and q is the probability of egress during one round of parasite replication (see Appendix). This model assumes the absence of proliferation - dependent egress, which is reasonable for sufficiently high values of q. The grey bars in Fig. 1B illustrate the model for values of q between 0.4 and 0.7; for these values, few parasites progress beyond five divisions.

We found that f_n declined rapidly for $n > 1$ (solid colored lines in Fig. 1B), in accord with the probabilistic model and in contrast to the even distribution expected for conventional proliferation-dependent egress. When vacuoles with greater than eight parasites were observed, they were almost always found in a cell population displaying the extensive basophilic cytoplasm characteristic of mesothelial cells (Fig. 1A b-c). These presumptive mesothelial cells constitute approximately ten percent of the recovered infected mononuclear cells, the remainder of which have a macrophage-like morphology (Fig. 1A a-b). In contrast to the distribution of P observed in total mononuclear cells, the distribution within the mesothelial component (blue dotted line in Fig. 1B) does not fit the probabilistic model but instead is consistent with conventional egress.

Since many of the infected macrophages (approximately 50 - 60 percent) bear multiple vacuoles, we also considered the possibility that egress occurs upon accumulation of a certain number of total parasites per cell, rather than a fixed number of parasite divisions. In this case, cells that bear more vacuoles should contain, on average, fewer parasites per vacuole. This, however, is not the case: vacuole progression was observed to be independent of cell vacuole number (Fig. S1).

Parasite transfer *in vivo* indicates the prevalence of early egress

The distribution data are suggestive of a distinct mode of egress in infected inflammatory macrophages. Alternatively, the findings might be explained by the progressive activation of antiparasitic function in infected macrophages. To directly assess the occurrence of early egress in the inflamed peritoneal cavity, we carried out adoptive transfer experiments to determine the rate of parasite egress from exudate cells *in situ.* Mice were infected intraperitoneally with transgenic parasites expressing either GFP or YFP (GFP-RH or YFP-RH). At day 5 post-infection, when ascites volume is approximately one ml, exudate was withdrawn from GFP-RH-infected live donor mice (injected one hour previously with Hoechst 33342 to label donor cells) and 0.1 ml rapidly transferred to YFP-RH-infected hosts. A timed sequence of samples was obtained from each host to assess parasite transfer from donor to host cells *in situ* by flow cytometry (Fig 2). Reciprocal transfers were performed at the same time and gave similar results. This approach allowed us to readily designate parasites of either strain as either donor cell-associated, host cell-associated or extracellular (Fig. 2A, B; gating of extracellular parasites not shown). A pilot cell sorting experiment demonstrated that parasite fluorescence was linearly related to intracellular parasite content (Fig. S2), in confirmation of our earlier results (21). The fraction of donor parasites remaining donor cell-associated was then determined. As shown in Fig. 2C, this fraction declined exponentially, implying a first-order decay process with a half-life of approximately two hours. A composite regression performed on data from six experiments (employing a total of 13 donor and 38 host mice) yielded a half-life of 3.1 ± 0.3 hours ($r^2 = 0.87$). These kinetics suggest a process that is fairly uniform both over time and throughout the population of donor parasite-bearing donor cells. The total amount of donor parasite residing in the host declined only slightly over time (dashed lines in Fig. 2C), indicating that the decline in the fraction of donor cell-associated donor parasite was the consequence of rapid parasite transfer.

To confirm that this assay measures parasite transfer, rather than donor cells misidentified as host cells, we examined the intracellular parasite burdens of donor and host cells. At early timepoints, genuine egress of GFP-RH from donor cells, with subsequent reinvasion of host cells, is expected to result in host cells containing only one or two GFP-RH, whereas donor cells will have a greater GFP-RH burden, resembling that of parental donor cells. This prediction was verified (Fig. 2D). We similarly verified the converse prediction that the YFP-RH profile of the newly invaded host cells should be consistent with the YFP-RH profile of host cells rather than that of donor cells, which will not have acquired more than one or two YFP-RH (data not shown). The verification of these predictions establishes that the assay detected actual parasite transfer.

To confirm that the observed egress was a physiological process and not an artifact arising from cell transfer, we re-examined the data in order to compare the rates of egress in the donor → host and host → donor directions. To accomplish this, we derived an estimate of the egress rate as a linear approximation over a brief interval (between one and 3 to 4 hours post-transfer), by determining the amount of non-donor cell-associated donor parasite (NDAP) at these two time points. The NDAP value is the sum of the host cell-associated donor parasite burden and extracellular donor parasites, and is calculated by assuming that total peritoneal cellularity is unchanged over the brief interval. The gain in NDAP over the interval is divided by the donor

cell-associated donor parasite burden (DAP; mean of one and three hour values) to generate an egress rate value (donor → host) expressed as the percent of DAP egressing per hour. To estimate host → donor egress, the converse calculation is performed (i.e. the gain in non-host cell-associated host parasite as a percentage of the total amount of host cell-associated host parasite). However, in this case, to correct for the fact that most reinvasion events occur in host cells and are not scored, the value for the donor cell-associated host parasite burden is multiplied by the (host cell) / (donor cell) ratio (mean of 1 h and 3 h values). As shown in Table 1, good agreement was obtained for egress in the two directions, confirming the validity of the assay. As an additional control, we have obtained similar egress values in experiments in which the use of vital dye was avoided by employing host mice expressing transgenic ECFP from an actin promoter (data not shown). Furthermore, these egress rates are consistent with the modeling of egress based on vacuolar parasite content (Fig. 1B). For example, if the length of a parasite replication cycle is 6 hours, then probabilistic egress, with probability per cycle set at 0.7 or 0.6, would result in a parasite transfer half-life of 3.45 or 4.5 hours, respectively. In comparison, under the conventional model of proliferation-dependent egress, with c = 6 cycles, the half-life would be 18 hours.

Role of exudate macrophages in early egress

We next sought to determine the exudate cell types in which cycles of early egress and reinvasion were taking place. As expected, the cell type with the greatest parasite burden was the F4/80$^+$ macrophage, carrying approximately half the total burden in both donor and host cells (Fig. 3). In comparison, B and T lymphocyte populations each contributed about five percent of the burden. The remaining burden was approximately evenly divided between neutrophils and small F4/80$^+$ cells that are not included in the macrophage gate (data not shown). When the distribution of egressed donor parasite (NDAP) was examined at three hours post-transfer, the largest share was again found in host macrophages (Fig. 3), with approximately half of reinvasion events occurring in this cell type. It is notable that three hours of transfer, a duration less than one parasite replication cycle, is sufficient for the macrophage share of NDAP burden to achieve a value identical to the macrophage share of endogenous parasite. This finding suggests that parasite distribution may be governed less by preferential replication in specific cells than by the dynamics of egress and reinvasion.

The finding of high levels of reinvasion in macrophages suggested that early egress may also be prominent in this cell type. To test this idea, we followed the kinetics of donor cell disappearance after transfer. Consistent with the previous kinetic analysis of donor parasite transfer, donor cells in the host animal were lost with zero-order kinetics over the first eight hours post-transfer, with a half-life of 3.6 hours (Fig. 4A). Remaining cells then decayed at a slightly slower rate. Donor macrophages were lost at a faster rate than total donor cells (half-life of 2.0 hours), and this corresponded to a higher frequency of initial infection in this cell type: 73% of input donor macrophages were infected, compared to 41% for total donor cells. In contrast, when uninfected thioglycolate-elicited peritoneal macrophages (PEM) were labeled and transferred to hosts undergoing thioglycolate peritonitis, little donor cell loss was observed (Fig. 4B), as reported previously (22). Consistent with these findings, we observed that peritoneal recruitment of circulating myeloid leukocytes was greatly elevated in *T. gondii*-infected mice compared to mice with thioglycolate peritonitis (Fig. S3). When ^{51}Cr-labeled PEM were injected intraperitoneally in mice undergoing either thioglycolate- or *T. gondii*-induced peritonitis, no significant difference was observed with respect to appearance of label in the draining thoracic lymph nodes (< 1 percent of input label; data not shown), suggesting that rapid macrophage clearance in infected mice was not due to enhanced drainage.

The correspondence between the high frequency of macrophage infection and rapid macrophage turnover suggests that this turnover may be driven by parasite egress. If this is the

case, it would be expected that donor macrophages already infected at the time of transfer will be lost more rapidly than their uninfected counterparts. This prediction was tested by assuming that donor cells bearing donor parasite had acquired the parasite pre-transfer, since most post-transfer infection is with host parasite. As shown in Fig. 4C, donor parasite-bearing donor macrophages indeed decayed faster than donor parasite-negative cells (half-lives of 1.8 and 2.4 hours, respectively, over the first eight hours of transfer). We next asked whether the decay of the donor parasite-negative macrophages could potentially be accounted for by egress subsequent to invasion by host parasite after transfer. As shown in Fig. 4D, by three hours post-transfer, the frequency of donor macrophages bearing host parasite was nearly equal to the steady-state frequency of infection observed in host macrophages (dashed line). These data are consistent with an egress-dependent mechanism of cell loss for the preponderance of donor macrophages.

An *in vitro* model of externally-triggered egress

The demonstration of early egress from inflammatory macrophages *in vivo* suggested that egress might be triggered by components of the inflammatory environment. To address this issue, we sought to develop an *in vitro* assay in which regulation of the process could be studied. As a first step, we prepared 'donor' and 'host' mice as for the adoptive transfer assay, and then, instead of performing exudate transfer, assessed parasite transfer in *ex vivo* cultures in which these exudates had been combined. One hour of co-culture of a 1:1 mixture of washed exudate cells resulted in a substantial increase in NDAP (Fig. 5A). The gain in NDAP (that is, the combined gain in extracellular + host cell-associated donor parasites) was equal to 20 ± 1 percent of initial DAP, a value which becomes 42 ± 1 percent when corrected for presumed unscored reinvasion events occurring in donor cells. This result suggested that cellular elements of the exudate might be sufficient to generate early egress. To confirm that soluble factors in the exudate were not required for the *ex vivo* assay, we compared egress in co-culture of washed cells to mixtures of whole unseparated exudates (Fig. 5B). In this experiment, mixtures are 1:9 (donor:host). The lower egress values for whole exudates may be related to partial coagulation that occurs in unseparated samples, in spite of the use of anticoagulants (data not shown).

To ask whether early egress was triggered by exudate cells, we added these cells, prepared from mice infected with nonfluorescent *T. gondii* (WT-RH), to monolayers of YFP-RH-infected PEM. Timelapse imaging, performed both before and after addition of exudate cells, revealed that the addition of these cells induced egress in approximately 40 percent of infected PEM within 120 minutes (Fig. 6A - C and Videos 1, 2). This egress rate (approximately 20 percent/hour) is consistent with the rates observed *in vivo* (Table 1). Few egress events occurred prior to 20 - 30 minutes after addition of exudate cells (Fig. 6D), coinciding with the interval required for complete settling of these cells onto the monolayer (data not shown). Subsequently, the egress rate was relatively uniform over time, suggesting that the egress was not a transient response to the addition of exudate cells. Flow cytometric analysis indicated that the majority of the egressed parasites were associated with exudate cells, which were present in excess over PEM (data not shown). These data indicate that early egress can arise as an acute response to a microenvironmental stimulus. We refer to this phenomenon as externally-triggered egress (ETE).

We adopted the PEM-exudate cell co-culture system for further studies of ETE, with the modification that, in order to ensure quantitative cell recovery for flow cytometry, non-adherent conditions were used, although this entailed a reduction in egress rate (data not shown). To minimize loss of cells and parasites to aggregation in the non-adherent system, co-cultures were routinely performed in the presence of EDTA, which had a minimal effect on egress (data not shown). Even with this precaution, parasite loss of up to 20 percent was sometimes observed (as in Fig. 5A), limiting sensitivity for the detection of NDAP gain. We therefore chose to

quantify egress in the PEM-exudate co-culture experiments by determining the NDAP / (total parasite) fraction, which proved to be a more robust and sensitive indicator than the measurement of absolute NDAP gain. This NDAP fraction displayed a time-dependent increase during 60 minutes of PEM-exudate co-culture (Fig. S4).

A control experiment was performed in order to confirm that, in this non-adherent system, egress measured in this way reflected an exudate cell-dependent event, rather than simply an increased ability to detect reinvasions that, in the absence of exudate, occurred in PEM and were therefore not scored. To allow the detection of reinvasions in PEM as well as exudate cells, dye-labeled, YFP-RH-infected PEM were mixed with a 9-fold excess of unlabeled PEM infected with WT-RH. This 'base' mixture was then incubated either with or without excess exudate cells or, as additional controls, a similar excess of additional unlabeled PEM (either infected or uninfected). The results showed that, while there was indeed a detectable level of 'basal' egress and reinvasion in the absence of exudate cells, the addition of these cells led to a clear increase in egress from PEM (Fig. 6E). Furthermore, ETE in this system was not simply the result of increased total cell density, or the presence of a large number of infected macrophages, as the effect of exudate cells was not mimicked by excess infected or uninfected PEM.

We next sought to determine the exudate cell types responsible for triggering ETE. The ETE assay was performed using exudate exposed briefly to a magnet in the presence or absence (mock depletion) of Dynabead-coupled antibodies. The 1A8 antibody was used to deplete neutrophils (PMN) in preference to RBC-8C5, which we and others have found to react with macrophages in these exudates (21,23). Pilot experiments demonstrated that 1A8 identifies a $CD11b^+$ exudate population that is clearly distinguished from $F4/80^+$ cells (data not shown). Alternatively a combination of antibodies was used to simultaneously deplete neutrophils and T and B lymphocytes (Fig. 7A, B). Finally, F4/80 was used to used to deplete macrophages; however, it was only possible to deplete about one third of these cells (Fig. 7C, D). Neutrophil depletion had no effect on ETE, while the additional depletion of lymphocytes led to only a small decline (Fig 7E). However, partial depletion of F4/80+ macrophages was sufficient to reduce ETE by approximately one half. To achieve a more complete macrophage depletion, we exploited the finding that neutrophil depletion was without effect. Therefore we simultaneously depleted both macrophages and neutrophils using a combination of F4/80 and anti-CD11b, which reacts with both cell types. Neutrophil depletion with 1A8 served as a control. The combined depletion resulted in effective removal of macrophages (Fig. 7F), which led to a 74% reduction of ETE (Fig. 7G). These data implicate the inflammatory macrophage as a key mediator (as well as a principal target) of ETE, although other cell types may contribute.

Inhibitor studies of externally triggered egress

We next employed a panel of inhibitors to investigate the mechanistic basis of ETE. No consistent effect on ETE was observed using antagonists of reactive oxygen or nitrogen species (N-acetylcysteine [NAC] or L-NIL, respectively), or with cyclosporine A (CsA) or PPADS, which can protect macrophages from cell death pathways that act, respectively, via opening of the mitochondrial permeability transition pore or purinergic receptor activation (24-26)(Fig. 8A). Inhibition of either classical or novel protein kinase C signaling (using Go-6976 or rottlerin, respectively) was also without effect, as was inhibition of signaling through either ERK or JNK MAP kinases with, respectively, U0126 or Jnk Inhibitor II (Fig. 8A). We also observed no effect upon inhibition of either phosphatidylinositol 3-kinase / mTOR by wortmannin or G protein signaling by pertussis toxin (data not shown). In contrast, ETE was reduced by 69 percent in the presence of SB203580, an inhibitor of stress-sensitive kinases of the MAPK family in both *Toxoplasma* and mammalian cells (27,28) (Fig. 8A). Furthermore,

chelation of intracellular calcium using BAPTA-AM strongly reduced ETE (Fig. 8B), consistent with previous reports describing the inhibition of inducible *T. gondii* egress with this compound (3,5,6). Therefore both stress-sensitive MAPK and calcium signaling are implicated in the generation of ETE. A recent report indicates that calcium-dependent *T. gondii* egress can be blocked by fluridone, an inhibitor of the synthesis of abscisic acid, a substance that controls intracellular calcium release (29). However, we observed little effect of fluridone on ETE (Fig. 8C), suggesting that alternative mediators of calcium release may govern this form of *Toxoplasma* egress.

To obtain more definitive evidence for the effect of SB203580 on ETE, timelapse experiments were performed to directly compare the rates of exudate-dependent egress in the presence or absence of the inhibitor. The results showed that the inhibitor profoundly blocked ETE, reducing the frequency of egress in infected PEM by 83 percent (Fig. 9A - C, Videos 2, 3). To confirm this finding in a more physiological setting, we determined the effect of SB203580 on egress in an *ex vivo* culture of mixed exudates. We again observed a marked reduction of egress by the inhibitor (Fig. 9D). Over the course of three such experiments, the inhibition observed was always at least 80 percent.

Closer examination of the timelapse images revealed that residual egress events in SB203580-treated co-cultures had distinct features (Fig. 10). In control cultures, vacuole disruption was, as expected, closely followed by parasite dispersal from the host cell, so that the entire process was always completed within one ten minute interval. In contrast, in the presence of the inhibitor, there was typically a substantial delay between vacuole disruption and parasite dispersal, allowing these two events to be separately visualized in images ten minutes apart. In approximately ten percent of these events, dispersal failed to occur during the interval of observation, suggesting arrest at the disruption stage (SB Cell-3 in Fig. 10). These data suggest that the inhibitor may affect one or more parasite functions required for the efficient execution of egress.

In vivo fate of egressed *T. gondii*

We next sought evidence for a potential impact of the egress - reinvasion cycle on *T. gondii* pathogenesis. Use of SB203580 for this purpose was problematic, as this inhibitor can also suppress *Toxoplasma* growth (30). We therefore performed an experiment to compare the fate of exudate parasites residing in either the intracellular (non-egressed) or extracellular (recently egressed) compartments. We first identified conditions of brief centrifugation of exudate cells that substantially pelleted intracellular but not extracellular parasites. A pool of exudates from YFP-RH-infected mice was then separated into aliquots that were either depleted by centrifugation or not (control). These aliquots, in which the intracellular proportion of total parasite burden was 10 percent or 93 percent, respectively, were transferred to WT-RH-infected hosts, and the recovery of total YFP-RH was then monitored by sequential peritoneal sampling and normalized to the recovery obtained at one hour post-transfer for each host animal. By one hour, parasites from the centrifuged aliquot had efficiently reinfected host cells: the cell-associated proportion of donor-derived parasites at this time point was 96 ± 0.4 percent for both aliquots (n = 5), indicating that parasites from the two aliquots were similarly viable and infectious. As in previous experiments, by three hours post-transfer, the majority of intracellular donor parasite had egressed from donor cells (data not shown). Therefore the 1 h to 3 h post-transfer interval represents the period in which parasites from the two aliquots exist in substantially different states: either primarily residing in cells of origin (control) or having just completed a cycle of egress and reinfection (centrifuged). In the subsequent intervals, on the other hand, the state of the two parasite populations is similar.

In accord with this kinetic of parasite distribution, we observed a fate difference between the two aliquots that was specific to the 1 h to 3 h interval (Fig. 11). The recovery of control

parasites following this interval was 50% greater than that of the centrifuged aliquot, but no further difference occurred subsequently. The overall recovery of control parasite was reduced in comparison to earlier adoptive transfer experiments (Fig. 2D). This is attributable to the need in this case to store exudate prior to transfer; we have observed that storage for one hour significantly reduces subsequent recovery (data not shown). The differential recovery of egressed and non-egressed parasites suggests that non-egressing parasites may survive and expand preferentially in comparison to an egressing parasite compartment, consistent with a potential role for ETE in host defense.

The reduced recovery of recently invaded parasites suggests that many exudate macrophages possess activated antiparasitic function. To verify this expectation, we examined the ability of cell-free exudate fluid to induce antiparasitic function in macrophages. The results demonstrated that pretreatment of PEM with exudate fluid was comparable in this respect to pretreatment with interferon-gamma (IFNγ, and that this activity was dependent on IFNγ signaling and nitric oxide generation (Fig. 12). Induction of nitric oxide production by exudate fluid was comparable to the level induced by IFNγ (data not shown). These data suggest that ETE could potentially act to limit parasite expansion by redistributing parasites to activated host macrophages (see Discussion and Fig. 13).

Discussion

The infective cycle of the tachyzoite form of *T. gondii* has been intensively investigated; however, studies to date have largely focused on elucidating the mechanisms of a fixed sequence of events, from invasion through replication and egress, rather than on the physiological regulation of these processes. It is indeed unclear how much regulation occurs for any of these events, either at the level of the parasite or initiated by the host. The current study provides evidence that, in the case of egress, physiological regulation may play a major role in shaping the progress of acute infection, with potentially significant consequences for host defense and pathogenesis.

A key finding of this study is that, in contrast to *in vitro* models of tachyzoite growth, in which the interval between parasite invasion and egress is typically 36 to 48 hours, in the macrophages that host a large fraction of the parasite burden during the acute inflammatory response this interval is dramatically shortened. Our data imply that a majority of the parasite residing in peritoneal exudate cells egresses approximately every 3 to 4 hours, and the kinetics of macrophage turnover suggest an even shorter interval (2 to 3 hours) for this cell type. Our conclusion that egress is a dominant event in this setting is based on four lines of evidence. First, the distribution of vacuolar parasite content in macrophages is consistent with a probabilistic, rather than proliferation-dependent model of egress. Second, rapid parasite transfer between donor and host cells is observed in adoptive transfer experiments. Third, the turnover of donor cells in these experiments is consistent with lytic egress as the mechanism of parasite transfer. Fourth, a similar rate of egress was induced in infected adherent macrophages co-cultured with exudate cells. The finding that donor-to-host parasite transfer continues to occur at a steady rate many hours after transfer, and that this transfer is mirrored by transfer at a similar rate from host to donor cells, strongly argues against an artifactual explanation for these observations.

Since *T. gondii* has been shown to egress efficiently in response to two cell death-inducing signals (Fas and perforin)(9), it is plausible that cytotoxic signals derived from activated leukocytes in the inflammatory exudate could provide the basis for high rates of egress *in vivo*. However, we found that the presence of lymphocytes was not necessary for ETE, arguing against a role for perforin. It remains possible that NK cell - derived perforin contributes to ETE. We have observed no consistent effect on ETE following magnetic depletion using the

NK antigens NK1.1 and DX5; however, these small cell populations were not sufficiently well distinguished for us to be certain of their efficient removal (data not shown). Since depletion of macrophages reduced ETE (whereas neutrophil depletion had no effect), our data are most consistent with the view that the inflammatory macrophage is the major inducing cell for ETE, as well as the major responding cell from which egress is initiated. Our data suggest that macrophages acquire ETE-inducing capability as a result of the activating environment in infected mice, since macrophages elicited by a sterile irritant (thioglycolate) were less effective ETE inducers. However, the nature of the upstream activating signals that elicit ETE-inducing function requires further investigation.

The mechanism by which macrophages trigger egress remains to be determined. Activated macrophages release Fas ligand, and are also capable of undergoing Fas-mediated death in certain circumstances (31,32). Immature monocytes are also susceptible to Fas-mediated death (33), and this susceptibility might be retained in many of the macrophages in the toxoplasmic exudate, since our data imply that these cells are predominantly recent emigrants. In addition, macrophages can release a variety of other mediators capable of triggering apoptosis, including reactive oxygen and nitrogen species. We have previously documented the occurrence of reactive oxygen - producing macrophages in the toxoplasmic inflammatory exudate (21), and we have also detected the progressive accumulation of nitric oxide in these exudates (data not shown). We have observed that 1 - 2 percent of the uninfected macrophages in the inflammatory exudate are TUNEL-positive, whereas infected cells are uniformly TUNEL-negative (20)(data not shown), so it is plausible that ETE represents a response to the induction of early stages of apoptosis (preceding endonuclease activation). However, our data do not support a role for reactive species-induced apoptosis in ETE, since we observed no inhibition of ETE with N-acetylcysteine or L-NIL. In addition, no inhibition was seen with cyclosporine, an inhibitor of the mitochondrial permeability transition pore that prevents apoptosis in many settings, including nitric oxide-mediated apoptosis in macrophages (24). We also failed to observe ETE inhibition by blockade of purinergic receptor signaling. We have attempted similar experiments using either soluble Fas ligand to assess the role of the Fas pathway or the pan-caspase inhibitor zVAD to more broadly address the role of apoptosis; however, each of these agents triggered significant egress in the absence of exudate, and the results were consequently inconclusive (data not shown). Further studies will be needed to more fully elucidate the role of apoptotic signaling in ETE.

Although the mechanism that governs ETE remains unknown, it is clear from our data that this mechanism includes a step that is highly and specifically sensitive to the MAPK inhibitor, SB203580. Importantly, the effect of SB203580 was validated in an *ex vivo* culture of mixed inflammatory exudates, eliminating the possibility that the result was an artifact of the ETE assay system. There are at least three sites at which this inhibitor might potentially exert its effect in the ETE assay: the triggering exudate cell (presumably a macrophage) which generates an ETE-inducing signal that acts on infected PEM; the host compartment of the target cell (PEM) within which parasites initiate egress; and the parasite itself. We are as yet unable to distinguish these possibilities, since SB203580 is a reversible inhibitor and can act on both mammalian p38 MAPK27 and a related *T. gondii* - encoded kinase, TgMAPK1 (28). Both of these kinases are capable of responding to external stress signals.

If the inhibitor exerts its effect by acting on p38 MAPK in the triggering cell, a potential mechanism is the inhibition of cytokine production, which can be blocked in macrophages by SB203580 at both the transcriptional and translational levels (34,35). An alternative mechanism, which might operate on both triggering and target cells, is the inhibition of cell locomotion and/or the formation of appropriate cell-cell contacts, as many studies have implicated p38 MAPK in the regulation of the cytoskeleton and the promotion of cell migration (27). We have not obtained direct evidence for a role of cell-cell interaction in ETE, because

the standard two-compartment assay used for this purpose is complicated by the fact that the triggering exudate cells also serve as a major destination for egressing parasites. However, it is noteworthy that we observed the efficiency of egress induction to be increased by approximately an order of magnitude when the target PEM were adherent (as in the timelapse experiments) rather than non-adherent, as in our standard ETE assay (compare Figs. 6C and 6E). Also, in the adherent system, egress induction continued for at least two hours of co-culture, whereas in the non-adherent system most of the observable events were limited to the first hour (data not shown). These observations are consistent with a role for substrate-facilitated migration and cell-cell interaction in ETE.

Alternatively, if the relevant inhibitor target is TgMAPK1, then the inhibition of ETE could be due to either an effect on regulatory signals that govern parasite commitment to egress or alternatively to a blockade in the execution of egress. It may be pertinent in this respect that we have noted some inhibition by SB203580 of PEM invasion by *T. gondii* (data not shown), which has also been reported by others in the monocytic cell line THP-1 (36). Although these invasion studies do not distinguish between SB203580 effects on host and parasite kinases, the findings are consistent with the notion that ETE inhibition occurs via a blockade in egress execution, since parasite egress and invasion share mechanistic features (3,7). The finding that residual egress in SB203580-treated cultures shows an abnormal delay between vacuole disruption and parasite dispersal is also supportive of an inhibitor effect in the execution phase. However, since recent evidence suggests that host plasma membrane disruption is not a simple consequence of parasite exit per se (7), delayed dispersal may also reflect alteration of a host, rather than parasite function. It will be of interest to determine more precisely the events that are delayed or abrogated by SB203580. If a fundamental execution step of egress is affected, it might be expected that conventional proliferation-dependent egress during cell culture would also be sensitive to SB203580; however, this is difficult to test since parasite replication is inhibited by the action of the drug on TgMAPK1 (30).

The mechanistic relationship between ETE and proliferation-dependent egress will be an important subject for future enquiry. Most studies of *T. gondii* egress have been restricted to egress events artificially induced by agents such as calcium ionophores, dithiothreitol or bacterial toxins. However, the recent work of Lavine and Arrizabalaga indicates that proliferation-dependent egress is likely driven by stress of the host cell membrane due to the growing parasitophorous vacuole, and is mechanistically distinct in several respects from artificially induced egress (10). In particular, a key feature common to all instances of artificially induced egress is dependence upon intracellular calcium, as evidenced by the prevention of egress with BAPTA-AM. Similar calcium-dependence has been recently observed for egress induced by the ligation of death receptors in infected B lymphoma cells (9). In contrast, Lavine and Arrizabalaga report that proliferation-dependent egress is completely resistant to BAPTA-AM. These findings throw into question the physiological relevance of the earlier mechanistic findings. The current study, however, shows that inducible egress occurs physiologically and that it is dependent on intracellular calcium, in this respect resembling egress induced artificially or via death receptors, rather than proliferation-dependent egress. It is possible, then, that ETE represents a mechanistically distinct egress program that can be regulated by the parasite in response to environmental cues. It is possible, for example, that macrophages as host cells provide a favorable environment for ETE, since infection of macrophages with RH strain *T. gondii* upregulates host cell p38 MAPK function in a calcium-dependent manner (37). It will be of interest to determine whether the induction of ETE is specific to certain host cell types, and also whether features of artificially induced egress, such as host cell permeabilization and potassium entry, contribute to the mechanism of physiological ETE. A feature of artificially induced egress that may not be shared with ETE is dependence on the calcium-dependent protein phosphatase calcineurin, since the calcineurin

inhibitor cyclosporine A, which blocks calcium ionophore-induced egress (6), had no effect on ETE.

Alternatively, it remains possible that all *T. gondii* egress is calcium-dependent. A recent study, employing the same parasite strain and host cell as Lavine and Arrizabalaga, indicates that proliferation-dependent *T. gondii* egress is controlled through the production of abscisic acid (29). This finding suggests that the egress pathway is a calcium-dependent process, since abscisic acid stimulates calcium release in plants and other species (38-40), and activates calcium-dependent secretion in *T. gondii* (29). It is possible that the BAPTA-AM-resistance of egress observed by Lavine and Arrizabalaga reflects a difference in the calcium concentration required for rapid responses to external triggers, in comparison to a process that occurs over 1 to 2 days. However, it is also possible that proliferation-dependent egress can occur by more than one mechanism. We did not detect abscisic acid-dependence of ETE, implying, at least, that the initiating signals upstream of calcium release are distinct for ETE and proliferation-dependent egress. Whether this is the case for downstream events remains a question for further investigation.

The notion that ETE represents an environmentally cued parasite response suggests that this form of egress has developed as an adaptation of the parasite, for example as a means to escape inhospitable or dying cells. It has been suggested that induced egress may favor dissemination in the face of an immune response (9). However, our results suggest a second scenario, not exclusive of the first, in which the benefit to the parasite, if any, comes at a price in the setting of acute inflammation. Our data indicate that parasites that have recently reinfected new cells after egress fare poorly compared to those that have maintained longer residence in their host cells. The simplest explanation for this finding is based on the likelihood of heterogeneity among host cells (Fig. 13). We have shown that the environment of the peritoneal exudate is capable of inducing antiparasitic activity through the interferon gamma - iNOS axis. Since we have also shown that most macrophages in the exudate are likely to be very recent emigrants from the circulation, with varying degrees of exposure to these activating stimuli, and since the parasite can suppress IFN gamma-mediated activating signals that only arrive after infection (41), it is likely that exudate macrophages are highly heterogeneous with respect to activation state and consequent permissiveness. Consistent with this idea, we have demonstrated the existence of a subpopulation of reactive oxygen-expressing macrophages that appear resistant to infection *in vivo* (21). Heterogeneity of permissiveness is in fact characteristic even of resident peritoneal macrophages in normal mice (42,43). Since parasites will expand preferentially in more hospitable cells, such cells will perforce contain a disproportionately high share of total parasite. Therefore, any process, such as ETE, that tends to randomize parasite distribution will result in a net shift of parasite from more to less hospitable host cells, with benefit to the host. Such a host strategy of ‘haven disruption’ could in principle provide benefit in any setting in which an intracellular parasite was subject to an inducible release-reinfection cycle. The ultimate balance between parasite and host benefit might then depend on the signaling context of the setting in which egress was induced.

These considerations suggest that externally triggered egress may potentially contribute both to parasite expansion and to host defense. The ability to manipulate and exploit this modality of parasite transmission may therefore yield multiple avenues of investigation and intervention in *Toxoplasma* pathogenesis. In particular, the view of *T. gondii* egress as a microenvironmentally regulated event promises to provide further insight into the emerging picture of host-parasite interaction as a coevolved and highly adapted network.

Supplementary Material

Refer to Web version on PubMed Central for supplementary material.

Acknowledgments

The authors wish to thank Yanfen Ma for assistance with *T. gondii* culture, Jiu-feng Li for assistance with tail vein injections, and Michael Cammer and the Analytical Imaging Facility of the Albert Einstein College of Medicine for assistance with timelapse imaging.

Appendix

Probabilistic egress model

A theoretical distribution for parasite proliferation value (P) under the model of probabilistic egress (Fig. 1B) is derived as follows:

It is assumed that initially all parasite cycles are synchronous, and that all egress occurs at the parasite cycle midpoint (since egress is assumed to be unbiased with respect to cycle stage). We then consider two distributions: Dm(g) is the distribution of P immediately following the completion of the mid-cycle egress+reinvasion process in parasite generation g. Dc(g) is the distribution of P immediately following parasite division after the completion of generation g. A value for Dm or Dc has the form $(f_n) = (f_0, f_1 \ldots)$, where f_n = the fraction of total parasite for which P = n.

Suppose that for g = a, $Dm(a) = (m_0, m_1 \ldots)$.

Then $Dc(a) = (0, m_0, m_1 \ldots)$ (since all vacuoles now have at least two parasites).

It follows that: $Dm(a+1) = (q, (1-q)m_0, (1-q)m_1 \ldots)$, where q is the probability of egress.

Iteration then yields the series:

$$\begin{aligned} Dm(a+1) &= (q \quad , \quad (1-q)\,m_0 \quad , \quad (1-q)\,m_1 \quad \ldots) \\ Dm(a+2) &= \left(q \quad , \quad (1-q)\,q \quad , \quad (1-q)^2 m_0 \quad , \quad (1-q)^2 m_1 \cdots\right) \\ Dm(a+3) &= \left(q \quad , \quad (1-q)\,q \quad , \quad (1-q)^2 q \quad , \quad (1-q)^3 m_0 \ldots\right) \end{aligned}$$

It is then evident by induction that:

$$\begin{aligned} & Dm(g) = (q(1-q)^n) \\ \text{and} \quad & Dc(g) = \left(0, q(1-q)^{n-1}\right) \end{aligned}$$

Since Dm and Dc represent distributions that occur over equal time intervals (one half cycle each), the asynchronous distribution D is their mean:

$$D = \left(0.5q, 0.5\left(q(1-q)^n + q(1-q)^{n-1}\right), \quad \ldots\right)$$

References

1. Yap GS, Shaw MH, Ling Y, Sher A. Genetic analysis of host resistance to intracellular pathogens: lessons from studies of *Toxoplasma gondii* infection. Microbes Infect 2006;8:1174–1178. [PubMed: 16513380]
2. Black MW, Boothroyd JC. Lytic cycle of *Toxoplasma gondii*. Microbiol. Mol. Biol. R 2000;64:607–23.

3. Black MW, Arrizabalaga G, Boothroyd JC. Ionophore-resistant mutants of *Toxoplasma gondii* reveal host cell permeabilization as an early event in egress. Mol. Cell. Biol 2000;20:9399–9408. [PubMed: 11094090]
4. Silverman JA, Qi HL, Riehl A, Beckers C, Nakaar V, Joiner KA. Induced activation of the *Toxoplasma gondii* nucleoside triphosphate hydrolase leads to depletion of host cell ATP levels and rapid exit of intracellular parasites from infected cells. J. Biol. Chem 1998;273:12352–12359. [PubMed: 9575188]
5. Stommel EW, Ely KH, Schwartzman JD, Kasper LH. *Toxoplasma gondii*: Dithiol-induced Ca2+ flux causes egress of parasites from the parasitophorous vacuole. Exp. Parasitol 1997;87:88–97. [PubMed: 9326884]
6. Moudy R, Manning TJ, Beckers CJ. The loss of cytoplasmic potassium upon host cell breakdown triggers egress of *Toxoplasma gondii*. J. Biol. Chem 2001;276:41492–41501. [PubMed: 11526113]
7. Caldas LA, de Souza W, Attias M. Calcium ionophore-induced egress of *Toxoplasma gondii* shortly after host cell invasion. Vet. Parasitol 2007;147:210–220. [PubMed: 17560036]
8. Arrizabalaga G, Ruiz F, Moreno S, Boothroyd JC. Ionophore-resistant mutant of *Toxoplasma gondii* reveals involvement of a sodium/hydrogen exchanger in calcium regulation. J. Cell. Biol 2004;165:653–662. [PubMed: 15173192]
9. Persson EK, Agnarson AM, Lambert H, Hitziger N, Yagita H, Chambers BJ, Barragan A, Grandien A. Death receptor ligation or exposure to perforin trigger rapid egress of the intracellular parasite *Toxoplasma gondii*. J. Immunol 2007;179:8357–8365. [PubMed: 18056381]
10. Lavine MD, Arrizabalaga G. Exit from host cells by the pathogenic parasite *Toxoplasma gondii* does not require motility. Eukaryot. Cell 2008;7:131–140. [PubMed: 17993573]
11. Weiss LM, Laplace D, Takvorian PM, Tanowitz HB, Cali A, Wittner M. A cell culture system for study of the development of *Toxoplasma gondii* bradyzoites. J. Eukaryot. Microbiol 1995;42:150–157. [PubMed: 7757057]
12. Ma YF, Zhang YW, Kim K, Weiss LM. Identification and characterisation of a regulatory region in the *Toxoplasma gondii* hsp70 genomic locus. Int. J. Parasitol 2004;34:333–346. [PubMed: 15003494]
13. Gubbels MJ, Li C, Striepen B. High-throughput growth assay for *Toxoplasma gondii* using yellow fluorescent protein. Antimicrob. Agents Ch 2003;47:309–316.
14. Orlofsky A, Weiss LM, Kawachi N, Prystowsky MB. Deficiency in the anti-apoptotic protein A1-a results in a diminished acute inflammatory response. J. Immunol 2002;168:1840–1846. [PubMed: 11823517]
15. Hitziger N, Dellacasa I, Albiger B, Barragan A. Dissemination of *Toxoplasma gondii* to immunoprivileged organs and role of Toll/interleukin-1 receptor signalling for host resistance assessed by in vivo bioluminescence imaging. Cell. Microbiol 2005;7:837–848. [PubMed: 15888086]
16. Saeij JPJ, Boyle JP, Grigg ME, Arrizabalaga G, Boothroyd JC. Bioluminescence imaging of *Toxoplasma gondii* infection in living mice reveals dramatic differences between strains. Infect. Immun 2005;73:695–702. [PubMed: 15664907]
17. Orlofsky A, Somogyi RD, Weiss LM, Prystowsky MB. The murine antiapoptotic protein A1 is induced in inflammatory macrophages and constitutively expressed in neutrophils. J. Immunol 1999;163:412–419. [PubMed: 10384143]
18. Zenner L, Darcy F, Capron A, Cesbron-Delauw MF. *Toxoplasma gondii*: Kinetics of the dissemination in the host tissues during the acute phase of infection of mice and rats. Exp. Parasitol 1998;90:86–94. [PubMed: 9709034]
19. Mordue DG, Monroy F, La Regina M, Dinarello CA, Sibley LD. Acute toxoplasmosis leads to lethal overproduction of Th1 cytokines. J. Immunol 2001;167:4574–4584. [PubMed: 11591786]
20. Orlofsky A, Weiss LM, Kawachi N, Prystowsky MB. Deficiency in the anti-apoptotic protein A1-a results in a diminished acute inflammatory response. J. Immunol 2002;168:1840–1846. [PubMed: 11823517]
21. Shrestha SP, Tomita T, Weiss LM, Orlofsky A. Proliferation of *Toxoplasma gondii* in inflammatory macrophages in vivo is associated with diminished oxygen radical production in the host cell. Int. J. Parasitol 2006;36:433–441. [PubMed: 16516217]

22. Bellingan GJ, Caldwell H, Howie SEM, Dransfield I, Haslett C. In vivo fate of the inflammatory macrophage during the resolution of inflammation - Inflammatory macrophages do not die locally, but emigrate to the draining lymph nodes. J. Immunol 1996;157:2577–2585. [PubMed: 8805660]

23. Mordue DG, Sibley LD. A novel population of Gr-1(+)-activated macrophages induced during acute toxoplasmosis. J. Leuk. Biol 2003;74:1015–1025.

24. Hortelano S, Lopez-Collazo E, Bosca L. Protective effect of cyclosporin A and FK506 from nitric oxide-dependent apoptosis in activated macrophages. Br. J. Pharmacol 1999;126:1139–1146. [PubMed: 10205001]

25. Donnelly-Roberts DL, Namovic MT, Faltynek CR, Jarvis MF. Mitogen-activated protein kinase and caspase signaling pathways are required for P2X(7) receptor (P2X(7)R)-induced pore formation in human THP-1 cells. J. Pharmacol. Exp. Ther 2004;308:1053–1061. [PubMed: 14634045]

26. Mackenzie AB, Young MT, Adinolfi E, Surprenant A. Pseudoapoptosis induced by brief activation of ATP-gated P2X(7) receptors. J. Biol. Chem 2005;280:33968–33976. [PubMed: 15994333]

27. Cuenda A, Rousseau S. P38 MAP-Kinases pathway regulation, function and role in human diseases. BBA-Mol. Cell Res 2007;1773:1358–1375.

28. Brumlik MJ, Wei S, Finstad K, Nesbit J, Hyman LE, Lacey M, Burow ME, Curiel TJ. Identification of a novel mitogen-activated protein kinase in *Toxoplasma gondii*. Int. J. Parasitol 2004;34:1245–1254. [PubMed: 15491587]

29. Nagamune K, Hicks LM, Fux B, Brossier F, Chini EN, Sibley LD. Abscisic acid controls calcium-dependent egress and development in *Toxoplasma gondii*. Nature 2008;451:207–U11. [PubMed: 18185591]

30. Wei S, Marches F, Daniel B, Sonda S, Heidenreich K, Curiel T. Pyridinylimidazole p38 mitogen-activated protein kinase inhibitors block intracellular *Toxoplasma gondii* replication. Int. J. Parasitol 2002;32:969–977. [PubMed: 12076626]

31. Ashany D, Song X, Lacy E, Nikoliczugic J, Friedman SM, Elkon KB. Th1 Cd4+ Lymphocytes Delete Activated Macrophages Through the Fas/Apo-1 Antigen Pathway. Proc. Natl. Acad. Sci 1995;92:11225–11229. [PubMed: 7479970]

32. Fukui M, Imamura R, Umemura M, Kawabe T, Suda T. Pathogen-associated molecular patterns sensitize macrophages to Fas ligand-induced apoptosis and IL-1 beta release. J. Immunol 2003;171:1868–1874. [PubMed: 12902488]

33. Brown NJ, Hutcheson J, Bickel E, Scatizzi JC, Albee LD, Haines GK, Eslick J, Bradley K, Taricone E, Perlman H. Fas death receptor signaling represses monocyte numbers and macrophage activation *in vivo*. J. Immunol 2004;173:7584–7593. [PubMed: 15585886]

34. Brook M, Sully G, Clark AR, Saklatvala J. Regulation of tumour necrosis factor alpha mRNA stability by the mitogen-activated protein kinase p38 signalling cascade. FEBS Lett 2000;483:57–61. [PubMed: 11033356]

35. Lee JC, Laydon JT, Mcdonnell PC, Gallagher TF, Kumar S, Green D, Mcnulty D, Blumenthal MJ, Heys JR, Landvatter SW, Strickler JE, Mclaughlin MM, Siemens IR, Fisher SM, Livi GP, White JR, Adams JL, Young PR. A Protein-Kinase Involved in the Regulation of Inflammatory Cytokine Biosynthesis. Nature 1994;372:739–746. [PubMed: 7997261]

36. Gomez-Marin JE, Valere A, Bonhomme A, El'btaouri H, Antonicelli F, Burlet H, Aubert D, Villena I, Guenounou M, Haye B, Pinon JM. Interferon-gamma signal transduction during parasite infection: modulation of MAP kinases in the infection of human monocyte cells (THP1) by *Toxoplasma gondii*. Parasite Immunol 1998;20:631–635. [PubMed: 9990648]

37. Masek KS, Fiore J, Leitges M, Yan SF, Freedman BD, Hunter CA. Host cell Ca2+ and protein kinase C regulate innate recognition of *Toxoplasma gondii*. J. Cell Sci 2006;119:4565–4573. [PubMed: 17074836]

38. Wu Y, Kuzma J, Marechal E, Graeff R, Lee HC, Foster R, Chua NH. Abscisic acid signaling through cyclic ADP-Ribose in plants. Science 1997;278:2126–2130. [PubMed: 9405349]

39. Wasilewska A, Vlad F, Sirichandra C, Redko Y, Jammes F, Valon C, Frey NFD, Leung J. An update on abscisic acid signaling in plants and more. Mol. Plant 2008;1:198–217. [PubMed: 19825533]

40. Bruzzone S, Bodrato N, Usai C, Guida L, Moreschi I, Nano R, Antonioli B, Fruscione F, Magnone M, Scarfi S, De Flora A, Zocchi E. Abscisic Acid Is an Endogenous Stimulator of Insulin Release

from Human Pancreatic Islets with Cyclic ADP Ribose as Second Messenger. J. Biol. Chem 2008;283:32188–32197. [PubMed: 18784081]

41. Zimmermann S, Murray PJ, Heeg K, Dalpke AH. Induction of suppressor of cytokine signaling-1 by *Toxoplasma gondii* contributes to immune evasion in macrophages by blocking IFN-gamma signaling. J. Immunol 2006;176:1840–1847. [PubMed: 16424215]
42. Jones TC, Yeh S, Hirsch JG. The interaction between *Toxoplasma gondii* and mammalian cells. I. Mechanism of entry and intracellular fate of the parasite. J. Exp. Med 1972;136:1157–1172. [PubMed: 5082671]
43. Jones TC, Hirsch JG. The interaction between *Toxoplasma gondii* and mammalian cells. II. The absence of lysosomal fusion with phagocytic vacuoles containing living parasites. J .Exp. Med 1972;136:1173–1194. [PubMed: 4343243]

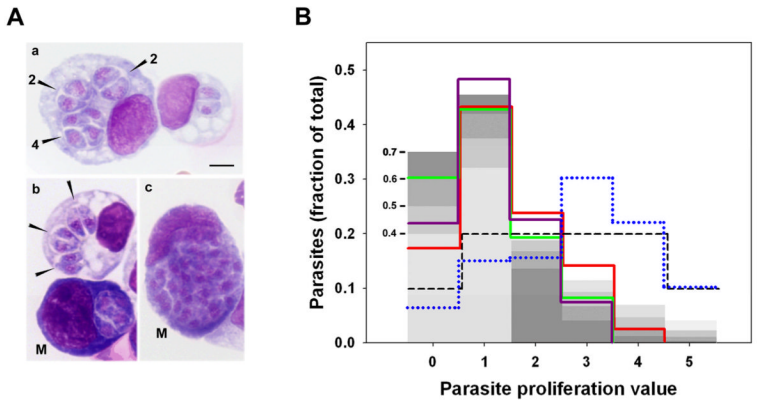

Figure 1. Distribution of intravacuolar parasite content in acute toxoplasmosis

Mice were infected intraperitoneally with *T. gondii* RH strain. **(A)** After 4 or 5 days, cytospin preparations of peritoneal exudate were Wright stained and parasitophorous vacuoles (arrowheads in a, b) were evaluated for parasite content. a, representative macrophages containing vacuoles in which 1 to 2 divisions have taken place (the number of parasites in each vacuole is indicated). b, an infected macrophage adjacent to an infected presumptive mesothelial cell (M). c, a mesothelial cell (M) with a vacuole bearing 32 parasites. Scale bar: 5 μm. **(B)** Parasite enumeration data were used to calculate the distribution of parasite proliferation value (the number of divisions within the vacuole for each parasite) in infected mononuclear cells. Each of the solid colored lines represents the distribution in total mononuclear cells from one mouse. For each sample, 300 - 400 vacuoles (approximately 600-800 total parasites) were scored. One sample (green line) is from d5 post-infection; the others are from d4. The data are representative of four total mice obtained from three independent experiments. The blue dotted line displays the distribution in mesothelial cells (pool of two mice from independent experiments; 87 total vacuoles, 376 total parasites assessed). The grey bars indicate the theoretical distribution under probabilistic egress, with each shade representing a different probability, as indicated by the numbers on the left (see text). The dashed line indicates the theoretical distribution for proliferation-dependent egress (see text).

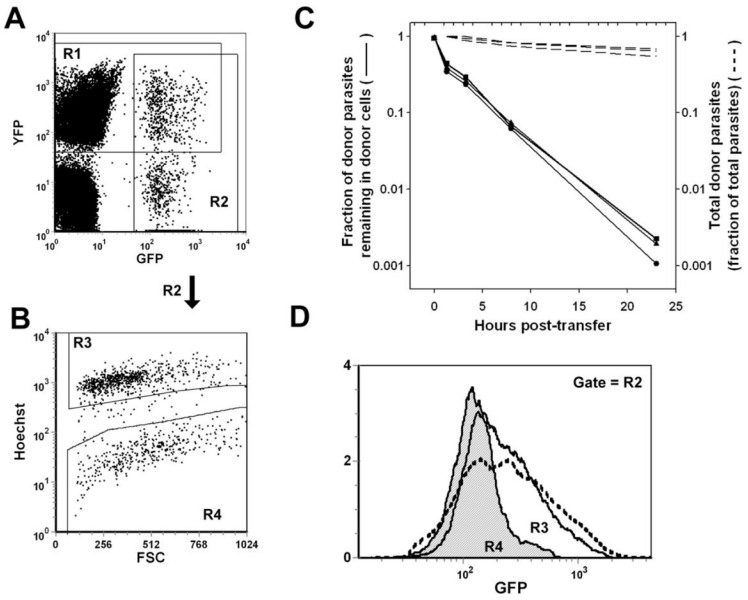

Figure 2. Transfer of parasite from donor to host cells *in vivo*

Donor peritoneal exudate was obtained by paracentesis from mice infected 5d earlier with either GFP-RH or YFP-RH and transferred immediately (0.1 ml/recipient) to host mice bearing a comparably progressed infection with the opposite strain. Donor cells were labeled *in situ* with Hoechst 33342 1 h prior to transfer. Host mice were sampled by paracentesis at the indicated times and the samples were analyzed by flow cytometry. **(A, B)** A sample taken 1 h after a GFP→YFP transfer is used to illustrate gating to distinguish host- and donor-derived parasite (gates R1 and R2, respectively, in (A)) and donor and host cells (gates R3 and R4, respectively, in (B), gated on R2). The dot plot in panel A is gated on total cells, exclusive of free parasites. In untransferred donor cells, the percentage of R2-gated cells present in R4 is < 1%. The uniformity and stability of Hoechst 33342 labeling is detailed in Fig. S5. **(C)** At each timepoint, the fraction of total donor parasite burden that remained donor cell-associated was calculated (solid lines). Each line represents sequential sampling of a single animal. The data are representative of 5 mice. The corresponding recoveries of total donor parasite (intracellular + extracellular, as a fraction of total parasites) are shown as dashed lines (the value at 1 h post-transfer is set to 1). **(D)** GFP-RH histograms of donor (unshaded, solid line) and host cells (shaded) 1 h after GFP→YFP transfer. A histogram of untransferred donor cells is shown for comparison (dashed line).

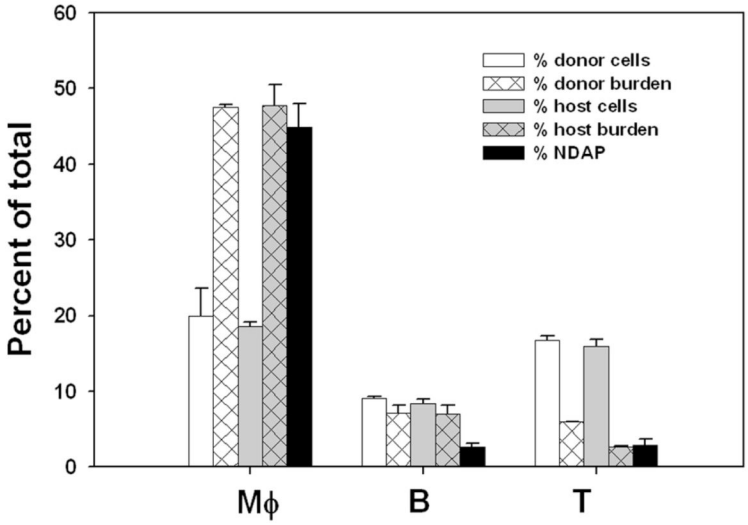

Figure 3. Cell type distribution of egressed parasites after reinvasion *in vivo*

Adoptive transfer was performed as in Fig. 2, using two donors (one each infected with YFP-RH or GFP-RH) and a total of five host mice. Samples were collected either before transfer (to determine donor cells and donor burden), 1 h post-transfer (to determine host cells and host burden), or 3 h post-transfer (to determine 'non donor-associated donor parasite' burden [NDAP]). The proportion of macrophages (Mφ), B and T cells was assessed for donor and host cells by flow cytometry after staining with antibodies against F4/80, B220 or Thy1. For each donor cell type, the fraction of total donor parasite residing in that population was determined (% donor burden), and, similarly, the fraction of total host parasite residing in each host cell type (% host burden). These distributions were then compared to the fraction of NDAP residing in each cell population. The data are representative of two experiments for lymphocytes and four experiments for macrophages.

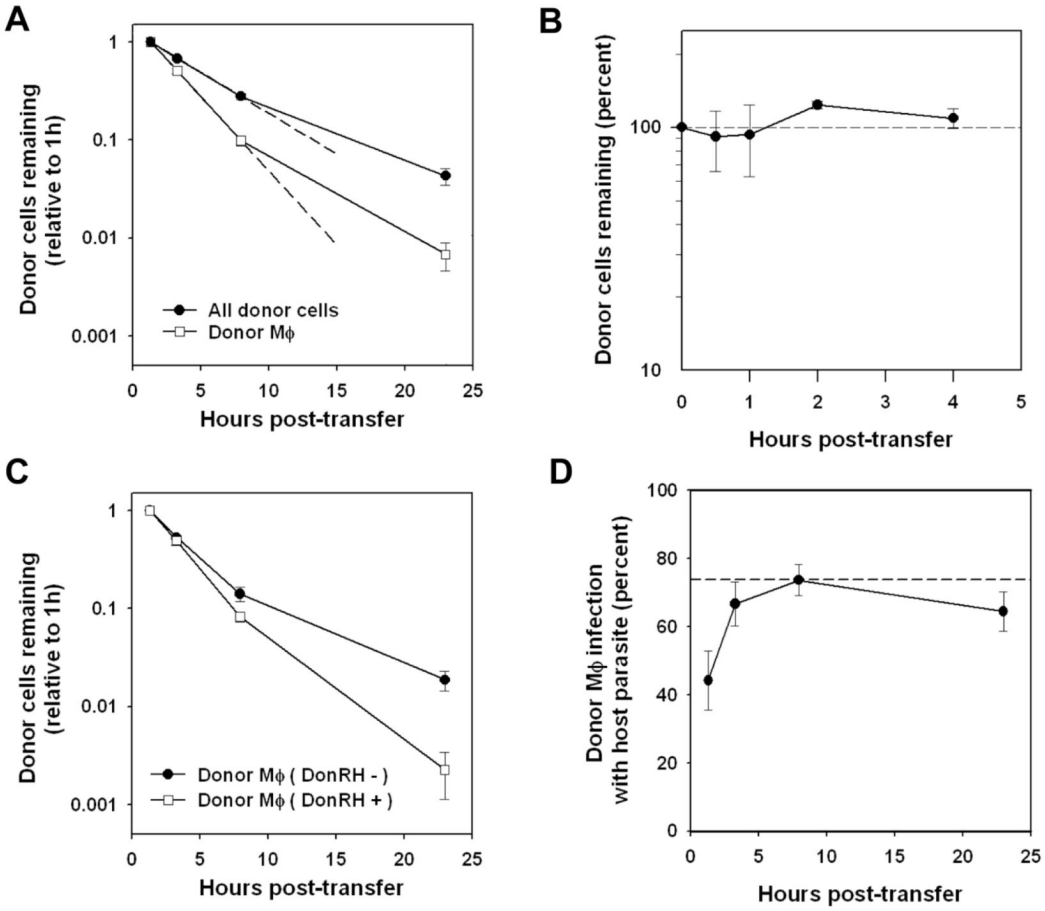

Figure 4. Kinetics of inflammatory cells in acute toxoplasmosis. (A, C, D)

Samples from the adoptive transfer described in Fig. 3 were stained with F4/80 to identify macrophages. Data are representative of 3 - 4 experiments **(A)** The recovery of donor macrophages and total donor cells (in each case as a ratio to total cells, relative to 1 h post-transfer) was determined by flow cytometry. Linear regressions (dashed lines) were calculated based on 1 h - 8 h data. **(B)** Donor and host mice were each injected intraperitoneally with thioglycolate. After 5d, donor exudate cells were harvested, labeled with CellTracker Orange, and injected into host mice. Groups of three mice were sacrificed at the indicated times to determine donor cell recovery. **(C)** Comparison of the recovery of donor macrophages infected or uninfected with donor parasites (reflecting infection status at the time of transfer). **(D)** The percent of donor macrophages infected with host parasite was monitored at the indicated times and compared to the frequency of host parasite infection of host macrophages (dashed line).

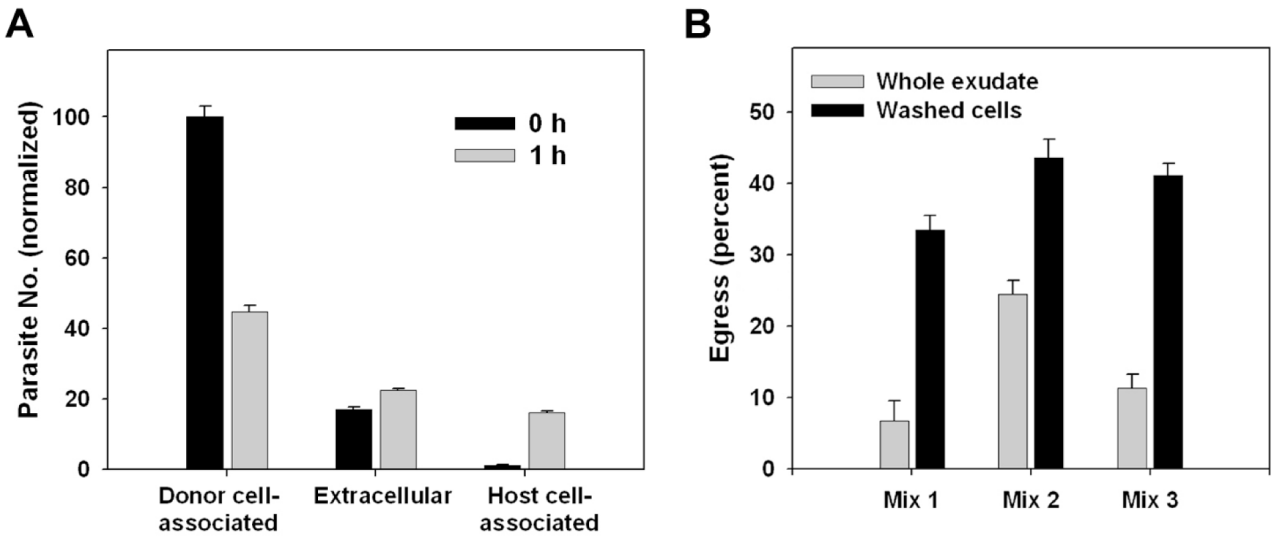

Figure 5. *Ex vivo* egress in toxoplasmic exudates

(A) Washed exudate cells ('host') prepared from mice 5d post-infection with GFP-RH were labeled *in situ* with Hoechst 33342 and mixed 1:1 with 'donor' exudate cells prepared from mice infected with YFP-RH. Each preparation represents a pool of 2 - 3 mice. Co-cultures were carried out for 1 h in non-adherent dishes in the presence of 1 mM EDTA + 10 U/ml heparin to reduce aggregation. The fate of donor YFP-RH was assessed by flow cytometry. The identity of donor and host cells bearing YFP-RH was verified by monitoring the intensity of GFP and YFP signals as discussed for Fig. 2 (not shown). The value for donor cell-associated parasites at 0 h was set to 100. **(B)** An experiment similar to (A) was carried out, except that co-cultures (1.5 h) of washed exudate cells were compared to similar co-cultures of whole exudate (fluid + cells). Instead of Hoechst dye, one exudate was labeled with DDAO-SE. The donor:host ratio was 1:9. Each of the 3 mixes represents a separate pair of donor and host mice. Whole exudate samples were filtered before analysis to remove any coagulated material. The data in the figure display mean ± S.E. of 3 replicates and are representative of either 7 (A) or 2 (B) similar experiments.

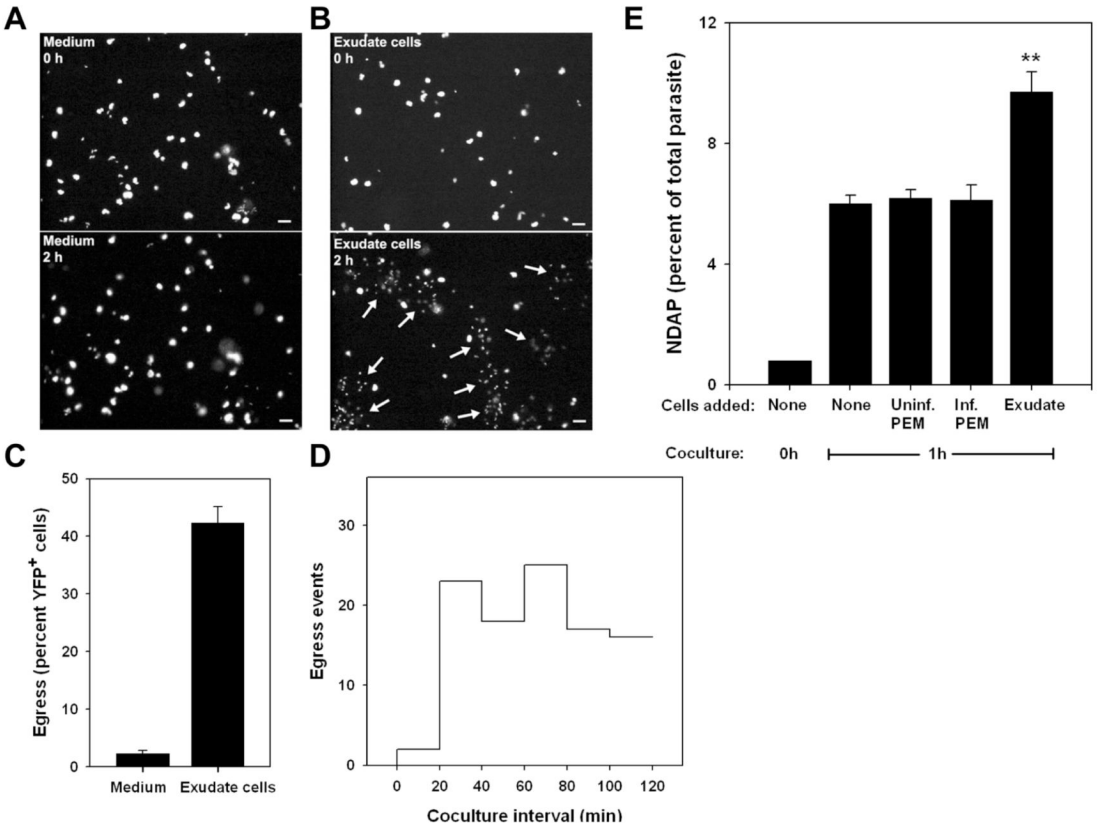

Figure 6. Externally-triggered egress *in vitro*

Egress was assessed in co-cultures of YFP-RH-infected thioglycolate-elicited macrophages (PEM) with washed exudate cells obtained from mice infected for 5d with wild-type RH. **(A, B)** YFP fluorescence is displayed from timelapse images (10 min intervals) of adherent PEM exposed at 0 h to either blank medium (A) or a 10-fold excess of exudate cells (B). Egress events that had occurred by 2h are indicated by arrows (lower panels). Scale bar: 20 μm. The quantitation of these egress events **(C)** represents the mean ± S.E. from either 3 (exudate) or 8 (medium) fields. The data are representative of two similar experiments. **(D)** The time distribution of exudate cell-induced egress events from the same experiment is displayed as a histogram. The settling of most exudate cells onto the PEM monolayer requires 15 - 20 min. **(E)** Flow cytometric assay of externally-triggered egress (ETE). Donor PEM infected overnight with YFP-RH (moi=0.2) were labeled with DDAO-SE and mixed (1:9) with PEM similarly infected with wild-type RH. Basal egress was then monitored by incubation of this mixture (None) for 1 h in non-adherent dishes, followed by determination of the percent YFP-RH not donor cell-associated (NDAP). ETE was measured as the additional NDAP generated by the addition of a 5-fold excess of washed exudate cells (Exudate). Control incubations were performed in the presence of a similar excess of uninfected or wild-type RH-infected PEM. ** $p < 0.01$ ($n = 4$). The data are representative of two similar experiments.

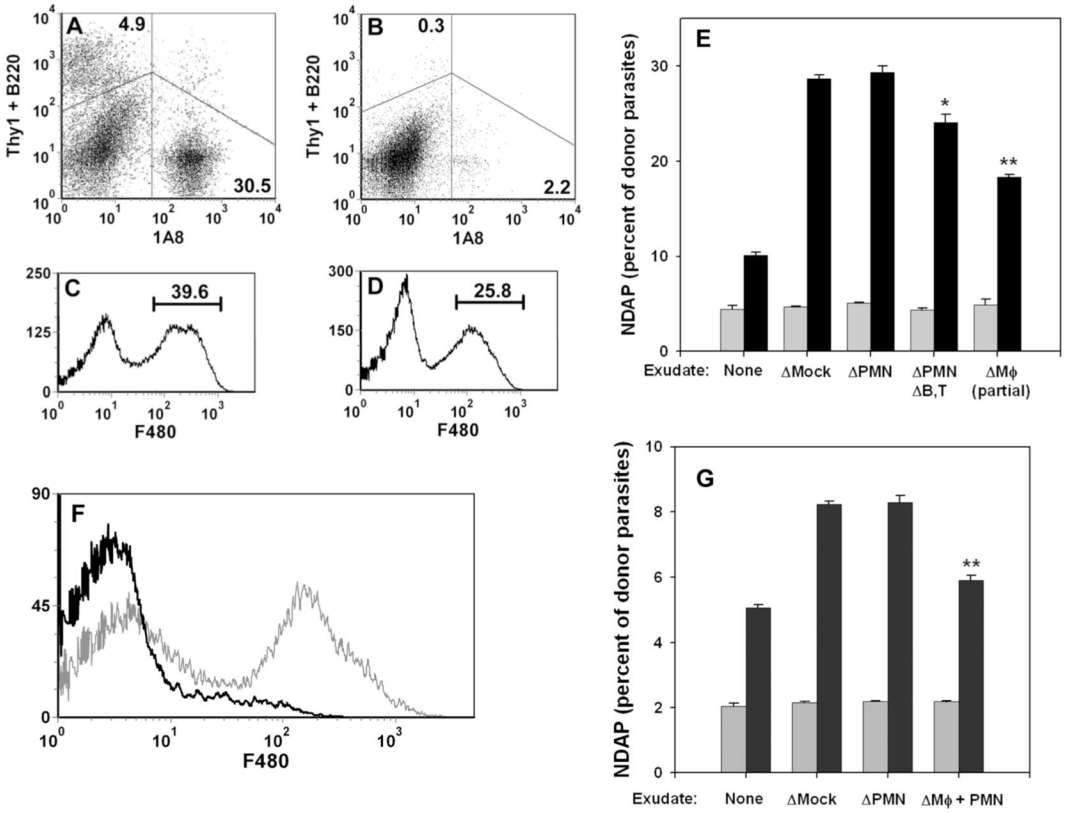

Figure 7. Role of exudate cell types in ETE

Exudate cells were prepared from mice infected for 5d with wild-type RH and depleted of specific cell types. In experiment 1 **(A - E)**, exudates were depleted of either 1A8+ cells (neutrophils), the combination of 1A8+ cells, B220+ cells and Thy1+ cells (neutrophil/B cell/T cell triple depletion), or F4/80+ cells (macrophages), or else mock-depleted. **(A, B)** Dot plots of cells triply stained with 1A8-PE/B220-APC/Thy1-APC antibodies, before **(A)** or after **(B)** depletion. Histograms of cells stained with F4/80 before **(C)** or after **(D)** depletion illustrate the partial depletion of macrophages. In experiment 2 **(F, G)**, exudates were depleted of either 1A8+ cells or the combination of CD11b+ cells and F4/80+ cells (neutrophil/macrophage double depletion). **(F)** Histogram of exudate cells stained with F4/80 before (grey) or after (black) double depletion of neutrophils and macrophages. **(E, G)** Donor PEM infected overnight with YFP-RH (moi = 1) were labeled with DDAO-SE and cultured for 1 h in non-adherent dishes with either medium (None) or a 5-fold excess of exudate cells depleted as indicated. NDAP (as percent of total donor parasites) was determined before (grey bars) and after (black bars) co-culture. Bars represent mean ± S.E. (n = 3). * $p < 0.05$. ** $p < 0.01$ (relative to mock depletion).

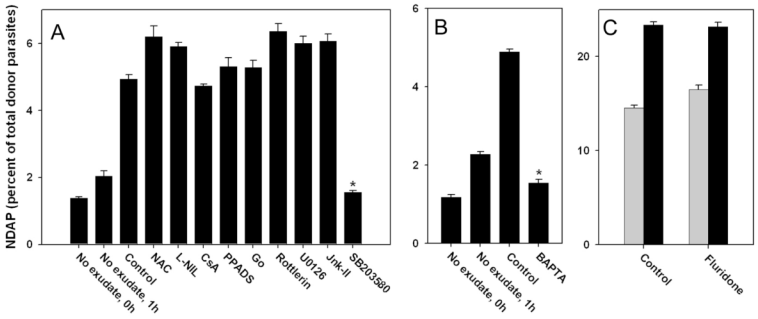

Figure 8. Effect of signaling inhibitors on ETE

ETE assays were performed as described for Fig. 7E. Bars represent mean ± S.E. (n = 4). **(A, B)** PEM were cultured with exudate in the absence (Control) or presence of the indicated inhibitors. The inhibitors used were N-acetylcysteine (NAC, 10 mM), L-NIL (1 mM), cyclosporine A (CsA, 5 μM), PPADS (30 μM), Go 6976 (Go, 1 μM), rottlerin (5 μM), U0126 (10 μM), JNK Inhibitor II (Jnk-II, 10 μM), SB203580 (10 uM), and BAPTA-AM (BAPTA, 10 μM). (A) and (B) represent separate experiments. * $p < 0.05$. **(C)** The ETE assay was performed on donor PEM that were first cultured overnight in either control medium (Control) or 50 uM fluridone, and then incubated in the absence (gray bars) or presence (black bars) of exudate. The data in the figure are representative of either 8 experiments (SB203580) or 2-3 experiments (other inhibitors).

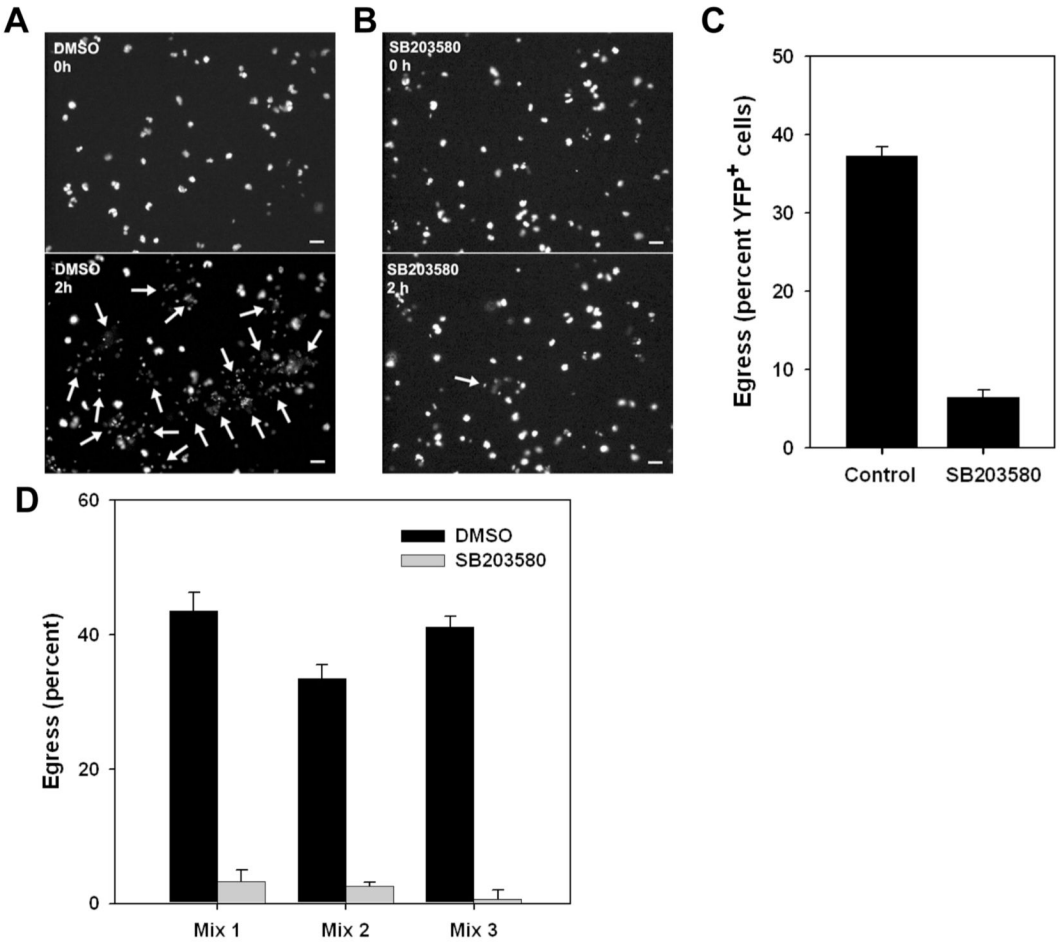

Figure 9. Inhibition of egress by SB203580

(A, B). YFP fluorescence in timelapse images (10 min intervals) of adherent PEM exposed at 0 h to exudate in the presence of either DMSO vehicle (A) or 10 uM SB203580 (B). Egress events that had occurred by 2h are indicated by arrows (lower panels). Scale bar: 20 μm. **(C)** The proportion of YFP-RH+ cells egressing over 2h is displayed as the mean ± S.E. from either 3 (DMSO) or 8 (SB203580) fields. The data are representative of two similar experiments. (D) Inhibition of egress in *ex vivo* mixed exudate. Washed donor exudate cells from mice infected for 5d with YFP-RH were labeled *in situ* with DDAO-SE, mixed (1:9) with unlabeled exudate from wild-type RH-infected mice, and incubated for 1 h in the presence of either vehicle or 10 uM SB203580. Each of the 3 mixes represents a separate pair of donor and host mice. Bars = mean ± S.E. (n = 3). The data are representative of three similar experiments.

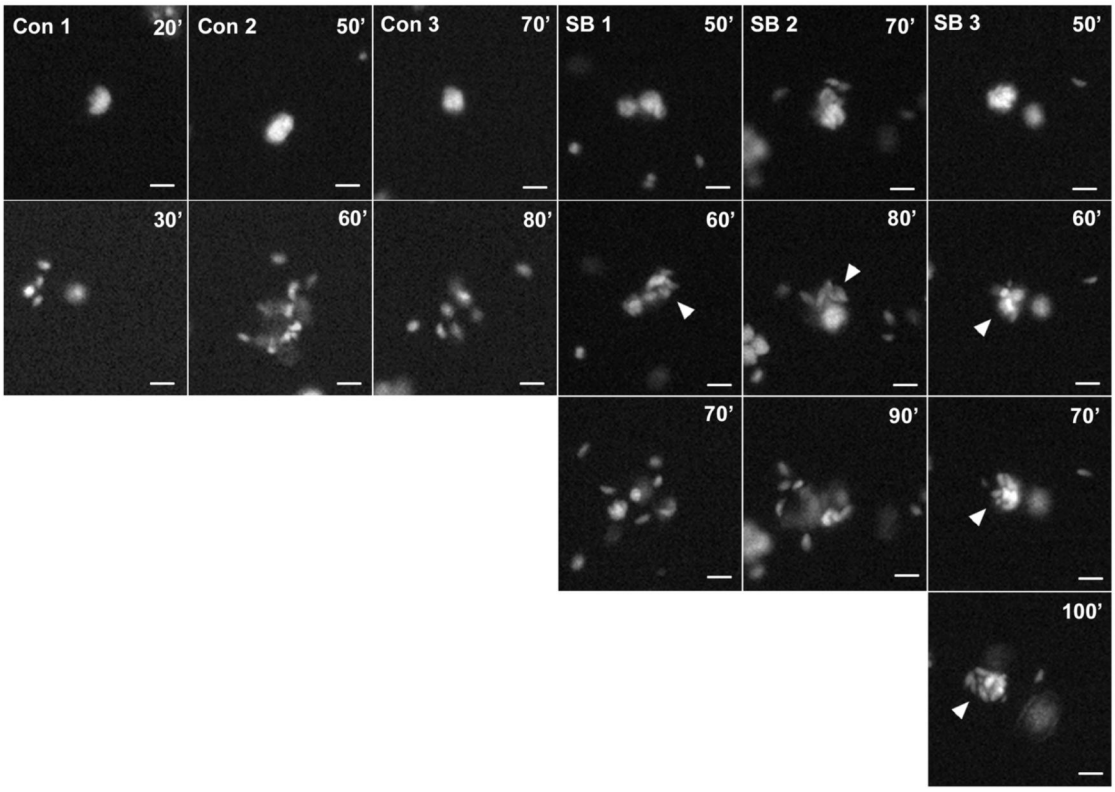

Figure 10. Altered progression of egress by SB203580

The timelapse series are from the experiment described in Fig. 9A,B. A random number generator was used to select 3 events each from the cultures treated with either DMSO (Con) (101 total events) or SB203580 (SB)(27 total events). Arrowheads indicate vacuoles that have undergone disruption but not dispersal. Scale bar: 10 μm.

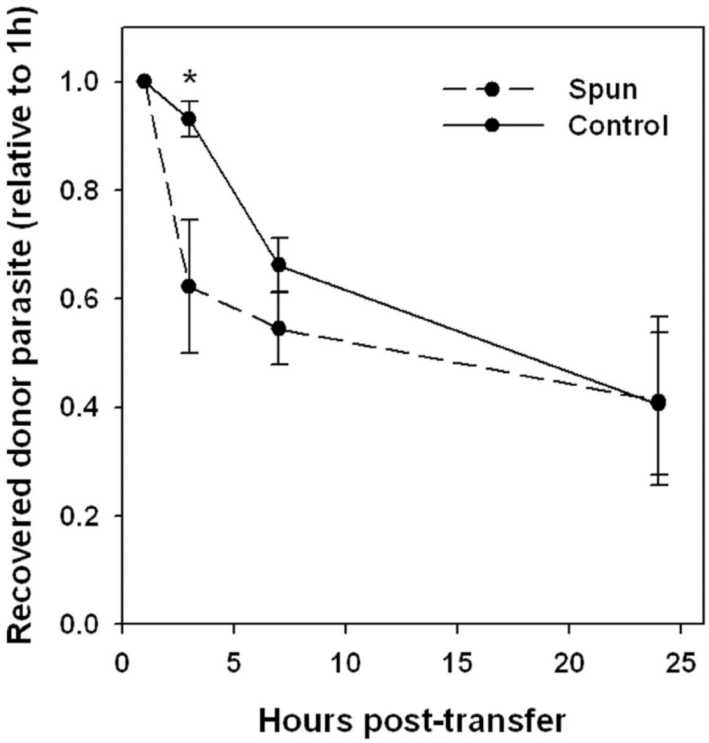

Figure 11. Fate of egressed parasites

Donor and host mice were infected for 5d with YFP-RH or wild-type RH, respectively. Exudates from 4 donors (verified to have similarly progressed toxoplasmosis) were pooled and divided into aliquots that were either centrifuged for 2 min (discarding the pellet) to enrich recently egressed parasites (Spun), or held at 4°C (Control). Each aliquot was transferred to a group of 5 host mice, of which 3 expressed transgenic CFP to mark host cells in order to monitor egress (not shown). Recovery of donor parasite was monitored by sequential paracentesis and normalized to the 1 h values for each host animal. * $p < 0.05$. The data are representative of two similar experiments.

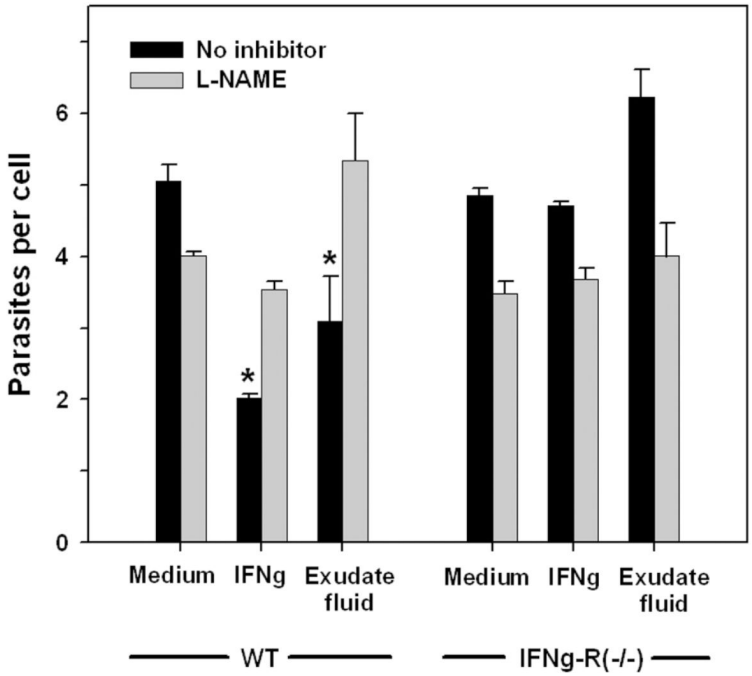

Figure 12. Activation of antiparasitic function by exudate fluid

Wild-type (WT) or IFNγR1$^{-/-}$PEM (1×10^5) were cultured for 1d in adherent 96-well dishes and then treated overnight with medium containing either 100 U/ml IFNγ, 20% cell-free exudate fluid prepared from infected mice (Exudate fluid), or no addition (Medium). Cells were then infected for 1d with GFP-RH at moi of either 0.1 or 2, in the presence or absence of the nitric oxide synthase inhibitor L-NAME (2.5 mg/ml). Data from the two infection levels were similar and were pooled for analysis. Cells were harvested by treatment with Accutase for 10 min and assessed for parasite content by flow cytometry, using fluorescent beads to normalize sample volume (n = 4). * $p < 0.05$. The data are representative of two experiments.

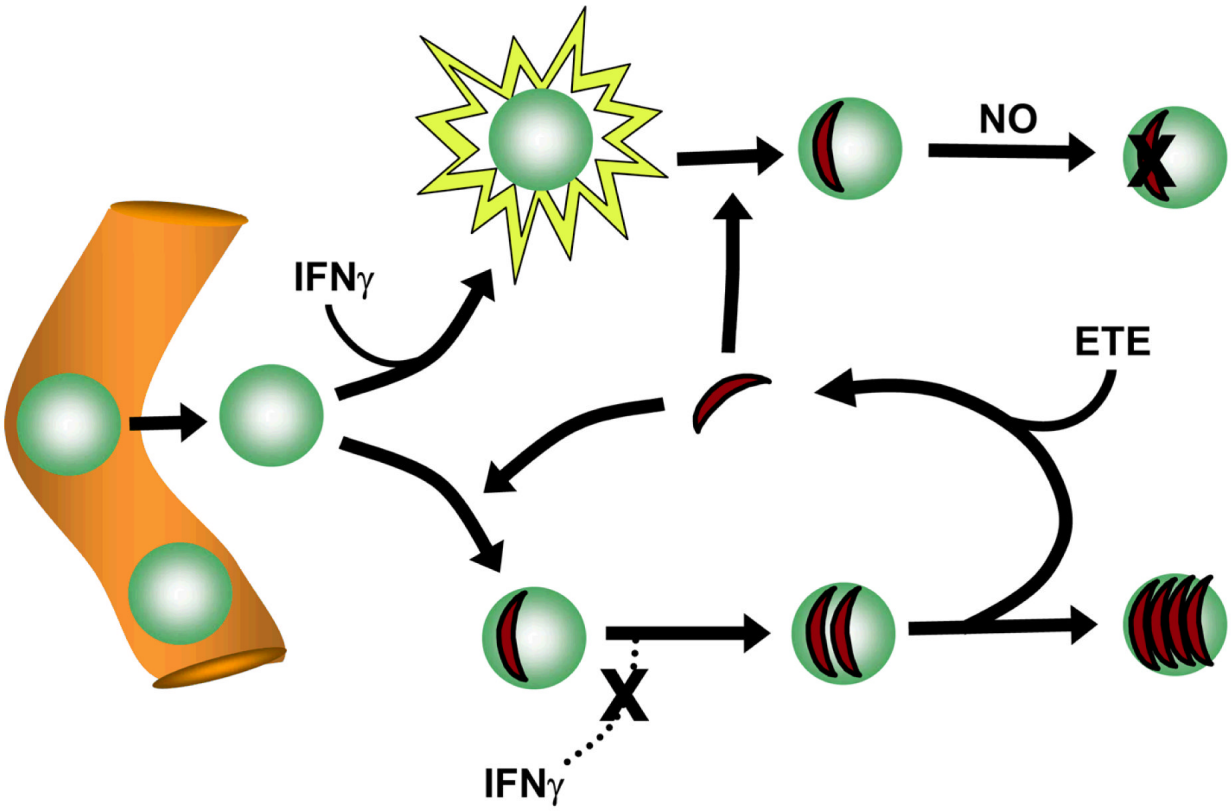

Figure 13. Hypothetical model for the role of ETE in host defense

Monocytes emigrating from blood vessels at a site of *T. gondii* infection encounter both activating signals, such as IFNγ, and parasites. The resulting macrophage is non-permissive if activation occurs first, since infection is followed by nitric oxide (NO) production, whereas it becomes relatively permissive (a 'haven') if infection occurs first, due to parasite-mediated suppression of IFNγ signaling. ETE forces parasite recycling from disrupted havens, resulting in a net transfer to non-permissive host cells that favors host defense.

Table 1

Comparison of egress rates from donor and host cells.*

Exp.	No. donor mice	No. host mice	Donor egress rate	Host egress rate
1	2	5	14 ± 2	12 ± 2
2	3	4	17 ± 4	18 ± 3
3	3	7	20 ± 4	8 ± 1

* Donor and host egress rates (percentage of parasites egressing per hour) are calculated similarly (see Methods), except that the host egress rate is multiplied by the (host cells)/(donor cells) ratio to correct for undetected reinvasion events occurring in host cells. Exp., experiment. No., number.